

Hydrogenation of 2-benzylpyridine over alumina-supported Ru catalysts: Use of Ru₃(CO)₁₂ as a Ru precursor



Tae Wan Kim^a, Jinho Oh^a, Young-Woong Suh^{a,b,*}

^a Department of Chemical Engineering, Hanyang University, Seoul 04763, Republic of Korea

^b Research Institute of Industrial Science, Hanyang University, Seoul 04763, Republic of Korea

ARTICLE INFO

Keywords:

Hydrogenation
2-Benzylpyridine
Triruthenium dodecacarbonyl
Thermal activation
Alumina

ABSTRACT

Although Ru₃(CO)₁₂ becomes a popular precursor for supported Ru catalysts nowadays, the activities of the catalysts prepared by thermolysis of the supported Ru₃(CO)₁₂ under different atmospheres have been rarely compared. We herein report the preparation of alumina-supported Ru samples by thermal activation of Ru₃(CO)₁₂ in air, H₂ or N₂, followed by activity test in the hydrogenation of 2-benzylpyridine (BPy). When the supported Ru₃(CO)₁₂ was activated in air, RuO₂ particles of 12–15 nm diameters were produced by complete oxidation of carbonyl groups. In contrast, thermal activation in H₂ and N₂ induced the formation of highly dispersed Ru⁰ particles of 1.4–2.3 nm diameters. In such activations methane was produced, suggesting that direct hydrogenation of CO coordinated to the Ru surface complex occurred in H₂ while the coordinated CO reacted with ruthenium hydride species in N₂. In the activity test for BPy hydrogenation, the samples prepared in H₂ and N₂ showed superior H₂ storage efficiencies and higher rate constants compared to those prepared in air (reduced before the reaction). Additionally, the former samples were examined to be relatively stable even though exposed to ambient air for 7 days. Therefore, H₂ and N₂ gases are recommended for thermal activation of alumina-supported Ru₃(CO)₁₂.

1. Introduction

In hydrogen storage regarded as an important issue in H₂ economy [1], the recently emerging solution is a liquid organic hydrogen carrier (LOHC) to store and release H₂ under relatively mild conditions showing a high H₂ storage capacity of 5–8 wt.% [2–5]. Most LOHC compounds consist of single or multi aromatic ring that can be hydrogenated into cyclic ring using renewable hydrogen. The H₂-rich LOHC of a liquid state is transported relatively easily and stored for a long term. At a H₂ unloading site, it is catalytically dehydrogenated into the H₂-lean form (also, a liquid) that will be reloaded at the original H₂ loading site or at a site to supply cheap H₂.

The challenging issue in LOHC system is to improve the dehydrogenation efficiency because the reaction is endothermic and thus favourable at high temperatures thermodynamically [5,6]; for instance, more than 270 °C is necessary for the hydrogenated form of (di)benzyltoluene [7]. To circumvent this intrinsic issue, the strategy of introducing N atom into the aromatic ring of LOHC has been developed, which significantly contributes to the decrease of dehydrogenation enthalpy [4,6,8]. However, this will have a negative effect on the Gibbs free energy of hydrogenation (ΔG_{HYD}) that is a backward reaction of

dehydrogenation, which is confirmed by comparing the calculated ΔG_{HYD} values between diphenylmethane vs. 2-benzylpyridine (Table S1; computation details in Supplementary materials). This is also verified by our preliminary results in the hydrogenation of the two substrates over supported Pt, Pd, Rh, and Ru catalysts: the selectivity to the full hydrogenation product is higher for diphenylmethane than for 2-benzylpyridine over each metal catalyst (Table S2). Thus, a study is necessary to find an active catalyst for the hydrogenation of N-containing LOHC; in this work, 2-benzylpyridine (BPy) is selected as a model LOHC. Note that BPy has a boiling point of 276 °C, a low melting point of 9 °C, and a hydrogen storage capacity of 6.7 wt.%.

The most frequently used catalysts for the hydrogenation reaction are supported noble metals such as Pt [9], Pd [10], Ru [11,12], and Rh [13]. In case of benzene hydrogenation, the activity decreased in the following order: Rh > Ru > Pt > Pd [14]. The similar order was observed in the hydrogenation of 1-methyl-2-pyrroleethanol [15] and 9-ethylcarbazole [16]; the order was Rh > Ru > Pd > Pt. However, there are very limited reports in literature for BPy hydrogenation: RuO₂ at 90–100 °C and 100 atm [17], and 5% Rh-on-carbon catalyst at 55–60 °C and 2.7 atm with 40% wt. ratio of the catalyst to the substrate [18]. In our preliminary test for BPy hydrogenation, Ru/Al₂O₃ showed

* Corresponding author at: Department of Chemical Engineering, Hanyang University, Seoul 04763, Republic of Korea. Tel.: +82 222202329; fax: +82 22202294.
E-mail address: ywsuh@hanyang.ac.kr (Y.-W. Suh).

Table 1
BPy hydrogenation activities and Ru⁰ particles sizes of the supported Ru catalysts.

Entry	Catalyst	Ru precursor	Activation condition	BPy conv. (%)	CHPI sel. (%)	BPI sel. (%)	CHPy sel. (%)	H ₂ storage eff. (%)	d (nm)
1	Pt/Al ₂ O ₃ ^{a,d}	–	–	98.7	23.8	75.7	0.5	61.1	–
2	Pd/Al ₂ O ₃ ^{b,d}	–	–	97.6	20.6	79.2	0.2	58.9	–
3	Rh/Al ₂ O ₃ ^{c,d}	–	–	81.9	15.2	83.7	2.6	47.2	–
4	Ru/Al ₂ O ₃ ^{c,d}	–	–	59.7	77.4	18.4	4.2	52.9	–
5	Ru(air-400) ^d	Ru ₃ (CO) ₁₂	Air at 400 °C	58.1	73.8	18.0	8.2	50.5	12.2
6	Ru(air-500) ^d	Ru ₃ (CO) ₁₂	Air at 500 °C	57.4	70.1	21.3	8.6	48.8	13.4
7	Ru(air-600) ^d	Ru ₃ (CO) ₁₂	Air at 600 °C	55.3	68.3	21.9	9.7	46.5	14.5
8	Ru(air-700) ^d	Ru ₃ (CO) ₁₂	Air at 700 °C	49.0	63.3	25.9	10.8	40.0	15.3
9	Ru(H ₂ -400)	Ru ₃ (CO) ₁₂	H ₂ at 400 °C	89.9	83.8	14.9	1.3	82.6	1.4
10	Ru(H ₂ -500)	Ru ₃ (CO) ₁₂	H ₂ at 500 °C	89.7	83.6	15.2	1.2	82.3	1.4
11	Ru(H ₂ -600)	Ru ₃ (CO) ₁₂	H ₂ at 600 °C	88.8	83.2	15.0	1.8	81.3	1.5
12	Ru(H ₂ -700)	Ru ₃ (CO) ₁₂	H ₂ at 700 °C	89.3	82.5	15.8	1.7	81.5	1.6
13	Ru(H ₂ -500) ^d	Ru ₃ (CO) ₁₂	H ₂ at 500 °C	89.5	81.4	16.1	2.5	81.2	1.4
14	Ru(H ₂ -500)	Ru(NO)(NO ₃) ₃	H ₂ at 500 °C	76.2	79.9	16.8	3.3	68.5	1.7
15	Ru(H ₂ -700)	Ru(NO)(NO ₃) ₃	H ₂ at 700 °C	77.8	76.9	17.9	2.2	68.9	2.0
16	Ru(N ₂ -400)	Ru ₃ (CO) ₁₂	N ₂ at 400 °C	86.3	82.3	16.1	1.6	78.6	1.4
17	Ru(N ₂ -500)	Ru ₃ (CO) ₁₂	N ₂ at 500 °C	86.8	82.5	16.2	1.3	79.5	1.4
18	Ru(N ₂ -600)	Ru ₃ (CO) ₁₂	N ₂ at 600 °C	82.0	80.8	17.4	1.8	74.2	1.7
19	Ru(N ₂ -700)	Ru ₃ (CO) ₁₂	N ₂ at 700 °C	82.1	80.3	17.8	1.9	74.0	2.3
20	Ru(N ₂ -500) ^d	Ru ₃ (CO) ₁₂	N ₂ at 500 °C	84.9	81.5	16.8	1.7	77.1	1.4
21	Ru(N ₂ -700) ^d	Ru ₃ (CO) ₁₂	N ₂ at 700 °C	79.6	79.0	19.1	1.9	71.3	2.3
22	Ru(H ₂ -500) ^e	Ru ₃ (CO) ₁₂	H ₂ at 500 °C	98.1	91.6	8.4	0.0	93.9	1.2
23	Ru(H ₂ -500) ^f	Ru ₃ (CO) ₁₂	H ₂ at 500 °C	99.0	91.7	8.3	0.0	94.8	1.2
24	Ru(N ₂ -500) ^e	Ru ₃ (CO) ₁₂	N ₂ at 500 °C	95.2	86.0	13.7	0.3	88.5	1.2
25	Ru(N ₂ -500) ^f	Ru ₃ (CO) ₁₂	N ₂ at 500 °C	91.9	86.4	13.0	0.6	85.6	1.2

^a 5 wt.% Pt/Al₂O₃ purchased from Sigma Aldrich.

^b 5 wt.% Pd/Al₂O₃ purchased from TCI chemicals.

^c 5 wt.% Rh/Al₂O₃ and 5 wt.% Ru/Al₂O₃ purchased from Alfa Aesar.

^d Reduced by H₂ at 250 °C for 3 h prior to the reaction.

^e Nominal Ru loading = 1 wt.%.

^f Nominal Ru loading = 3 wt.%.

the extremely high selectivity to the full hydrogenation product compared to Pt/Al₂O₃, Pd/Al₂O₃, and Rh/Al₂O₃ (Table 1, entries 1–4). However, the BPy conversion is significantly low over Ru/Al₂O₃. When we consider a very low price of Ru compared to Pt, Pd, and Rh, a highly active Ru catalyst needs to be developed for the efficient BPy hydrogenation.

Supported Ru catalysts have been generally prepared using RuCl₃ as a Ru precursor [12,19,20]. However, the chloride ion may remain in the final catalyst even after hydrogen reduction and additional washing [21,22]. To remove any negative effect of Cl[−], strong reducing agents such as hydrazine and sodium borohydride can be used [21–23], however, the synthesis process becomes more complicated. Another popular Ru precursor is Ru(NO)(NO₃)₃. It is well established in the literature that Ru(NO)(NO₃)₃ is converted to Ru metal particles by thermal activation in H₂ [24–26]. The other Ru precursor is triruthenium dodecacarbonyl Ru₃(CO)₁₂ that we have used in this work. It was reported that the higher Ru dispersion was attained over the catalyst prepared by Ru₃(CO)₁₂ among several Ru precursors [24,25]. In previous reports thermal treatment of supported Ru₃(CO)₁₂ catalysts was investigated under vacuum and hydrogen [27–45], and under inert gas [46,47]. Nevertheless, the activities of the catalysts prepared by thermolysis of the supported Ru₃(CO)₁₂ under different atmospheres have been rarely compared.

In this work the supported Ru₃(CO)₁₂ is decomposed in air, H₂, and N₂ at different temperatures ranging from 400 to 700 °C, where the support material is γ-Al₂O₃ that has Lewis acid sites useful for hydrogenation [48] and exhibits excellent thermal stability [49]. After the as-prepared or reduced samples are tested in BPy hydrogenation at 150 °C and 40 barg H₂, the activity results and the size of Ru⁰ particles are compared in order to suggest the optimum decomposition condition yielding an active Ru catalyst for BPy hydrogenation. Additionally, the effect of post-treatment on the activities of Ru catalysts prepared under H₂ and N₂ at 500 °C is investigated. Since this work focuses on the preparation of a supported Ru catalyst active for BPy hydrogenation

when Ru₃(CO)₁₂ is used as a Ru precursor, the results and discussion herein will be useful for the hydrogenation of N-containing LOHC over Ru catalyst and furthermore for the hydrogenation reactions demanding Ru as an active metal.

2. Experimental

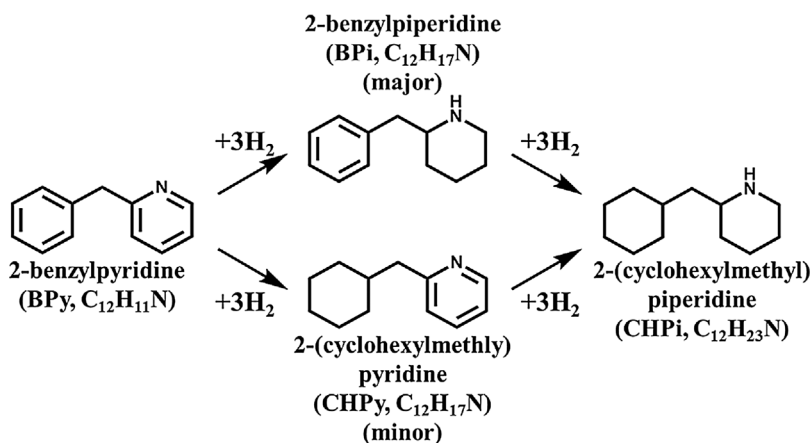
2.1. Preparation of Ru/Al₂O₃ samples by thermal decomposition of the supported Ru₃(CO)₁₂

Supported Ru catalysts were prepared by impregnating the as-received γ-Al₂O₃ support (Stream Chemicals, 216 m² g^{−1}) with a solution of Ru₃(CO)₁₂ (Sigma-Aldrich Chemical Co.) in tetrahydrofuran (Daejung Chemicals). After the suspension was stirred for 12 h at room temperature, the solvent was removed in a rotary evaporator (EYELA) under reduced pressure at 45 °C. The obtained sample was dried at 105 °C for 10 h. Finally, it was thermally treated at 400, 500, 600 or 700 °C in stagnant air, a H₂ flow (100 sccm) or a N₂ flow (100 sccm) for 5 h (ramping rate: 5 °C min^{−1}). Although the nominal Ru loading was 5 wt.% for all samples, the actual Ru loading was measured to be 4.43 wt.% in average by ICP-OES analysis. The final samples were referred to as Ru(X–Y) in which X is the activation gas (air, H₂ or N₂) and Y is the activation temperature in a unit of °C (400, 500, 600 or 700).

Additionally, Ru(H₂-500) and Ru(N₂-500) samples with the nominal Ru loadings of 1 and 3 wt.% were prepared by the method described above, where the actual Ru loadings were measured to be 0.72 and 2.23 wt.% in average for each loading.

2.2. Characterization of the prepared samples

Powder X-ray diffraction (PXRD) analysis was conducted with a Rigaku miniFlex300 diffractometer using a Cu Kα radiation source (30 kV and 10 mA). All diffraction patterns were recorded in 2θ range 10–90° at a scan rate of 5° min^{−1} in a step of 0.02°. Fourier-transform



Scheme 1. Reaction pathway in the hydrogenation of 2-benzylpyridine (BPy) into 2-(cyclohexylmethyl)-piperidine (CHPi) through two single-ring hydrogenation intermediates, 2-benzylpiperidine (BPi) and 2-(cyclohexylmethyl)pyridine (CHPy). Note that the pyridine ring is hydrogenated much faster than the benzene ring.

infrared (FT-IR) spectra of the as-impregnated sample and the activated samples were recorded with a Nicolet 6700 spectrometer (Thermo Scientific) equipped with a DTGS detector in the range 2200–1900 cm⁻¹ at the resolution of 8 cm⁻¹. Transmission electron microscopy (TEM) images were taken at a JEOL JEM-2100F microscope with an acceleration voltage of 200 kV, where the specimen was prepared by dropping the sample in ethanol onto a copper grid and subsequent drying in a vacuum at 40 °C. Ru composition was measured with an inductively coupled plasma optical emission spectrometer (ICP-OES) using an OPTIMA 8300 instrument (Perkin Elmer). For measurement of actual Ru loading, the activated sample was in contact with a mixture of aqua regia (5 ml) and distilled water (5 ml), followed by pretreatment in a microwave digestion system (Topex, PreeKem).

Temperature-programmed desorption experiments coupled with a mass spectrometry detector (TPD-MS) were performed to monitor the decomposition behaviour of the supported Ru₃(CO)₁₂ precursor. For experiments in an air flow (90 sccm), the sample (30 mg) was heated to 900 °C (ramping rate: 5 °C min⁻¹) in a NETZSCH TG209F1 instrument, while the mass signals of *m/z* = 18 and 44 for H₂O and CO₂, respectively, were measured using a NETZSCH QMS403C. For TPD-MS experiments in a flow of H₂, N₂ or He (30 sccm for all gases), the sample (50 mg) was heated to 900 °C (ramping rate: 5 °C min⁻¹) with a BELCAT-B instrument (BEL Japan, Inc.), while the mass signals of *m/z* = 16, 18, 28, 30, and 44 were measured using a BEL-Mass spectrometer to investigate evolution of CH₄, H₂O, CO, NO/NO₂/N₂O, and CO₂, respectively.

Temperature-programmed reduction (TPR) experiments were conducted in an AutoChem 2910 instrument (Micromeritics) by ramping to 600 °C (rate: 5 °C min⁻¹) in a 10% H₂/Ar flow (50 sccm), after the sample (50 mg) was in-situ pretreated in two different ways: (1) the sample was heated at 300 °C (ramping rate: 5 °C min⁻¹) for 1 h and then cooled to 50 °C, where the stream was an Ar flow (50 sccm) in the whole run and (2) the sample was heated at 400 °C (ramping rate: 5 °C min⁻¹) for 1 h in a 10% O₂/He flow (50 sccm) to oxidize Ru⁰ metal to RuO₂ and then cooled to 50 °C in an Ar flow (50 sccm).

CO chemisorption was carried out with a BELCAT-B instrument (BEL Japan, Inc.), where the sample (50 mg) was pretreated at 250 °C for 1 h (ramping rate: 5 °C min⁻¹) in a 10% H₂/Ar flow (30 sccm). After cooling to 30 °C in a He flow (30 sccm), 5% CO/He gas was repeatedly injected as a pulse until the peak area became saturated. The diameter of Ru⁰ particles (*d*) was calculated using a ChemMaster program (details in the Supporting Information), where a chemisorption stoichiometry CO/Ru was assumed to be 1:1.

2.3. Hydrogenation activity test

The hydrogenation reaction experiment was performed in a Parr reactor (volume 100 ml). Typically, the substrate BPy (3 g), the solvent

decalin (27 g), and supported Ru sample (catalyst 36, 72, and 222 mg for the actual Ru loading of 4.43, 2.23, and 0.72 wt.%, respectively) were added into the reactor, where the Ru/substrate ratio was constant at 0.089% in every run. This ratio was calculated as follows: [(catalyst weight × actual Ru loading/Ru atomic mass)/(BPy weight/molecular weight of BPy)] × 100. After the reactor was purged with N₂, H₂ was fed into the reactor up to 40 barg that was maintained throughout the reaction using a back pressure regulator. The reactor was then heated to 150 °C and as soon as the temperature reached 150 °C, the stirring started with a rate of ca. 400 rpm (reaction time *t* = 0). After the reaction for 2 h, the reactor was cooled to ambient temperature. The reaction temperature and time were chosen by preliminary results. When we conducted the hydrogenation experiments at 130, 150, and 170 °C, the activity difference at 150 °C appeared to be fairly good in comparing the catalytic performance of Ru(H₂-500), Ru(N₂-500), and Ru(air-500) samples (Fig. S1). Furthermore, when the BPy conversion and H₂ storage efficiency of the three samples at 150 °C were plotted against the reaction time, their increasing trend was changed around 120 min as the reaction approaches the maximum conversion (Fig. S2).

The reaction mixture was analysed with a Younglin YL6500 GC equipped with a flame ionization detector and an HP-5 column (30 m × 0.32 mm × 0.25 μm). The reaction pathway in BPy hydrogenation is depicted in Scheme 1. The BPy conversion and selectivities to CHPi, BPi, and CHPy were calculated by the following equations:

$$\text{BPy conversion (\%)} = 1 - \frac{\text{BPy mole}}{\text{BPy} + \text{BPi} + \text{CHPy} + \text{CHPi moles}} \times 100.$$

$$\text{CHPi selectivity (\%)} = \frac{\text{CHPi mole}}{\text{BPi} + \text{CHPy} + \text{CHPi moles}} \times 100.$$

$$\text{BPi selectivity (\%)} = \frac{\text{BPi mole}}{\text{BPi} + \text{CHPy} + \text{CHPi moles}} \times 100.$$

$$\text{CHPy selectivity (\%)} = \frac{\text{CHPy mole}}{\text{BPi} + \text{CHPy} + \text{CHPi moles}} \times 100.$$

Furthermore, the hydrogen storage efficiency was calculated as follows:

$$\text{H}_2 \text{ storage efficiency (\%)} = \frac{[\text{CHPi mole} \times 6\text{H}_2 + (\text{BPi} + \text{CHPy}) \text{ moles} \times 3\text{H}_2]}{(\text{BPy mole} \times 6\text{H}_2)} \times 100.$$

3. Results and discussion

3.1. Ru(air) samples prepared by thermal decomposition of the supported Ru₃(CO)₁₂ in air

Fig. 1a shows PXRD patterns of the as-prepared Ru(air) samples, indicating the major reflections corresponding to RuO₂ (PDF #43-1290)

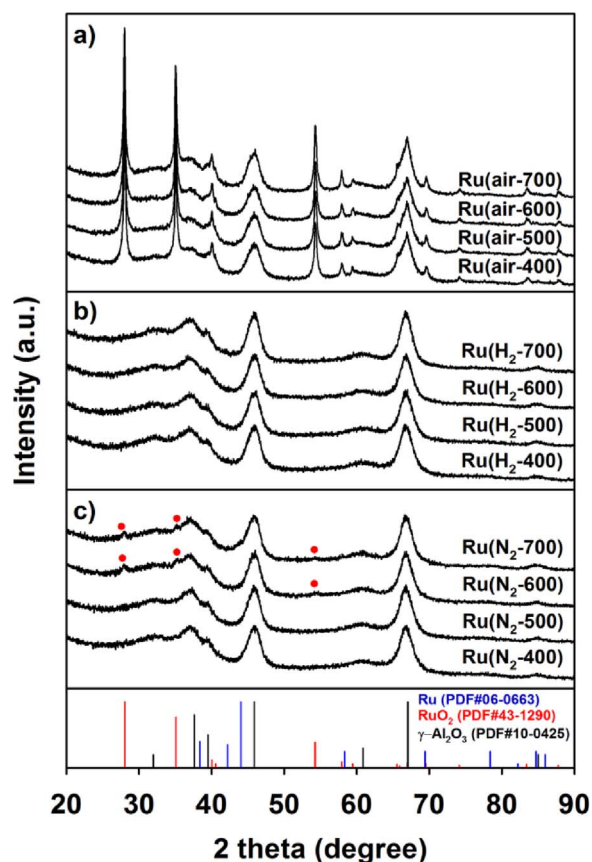
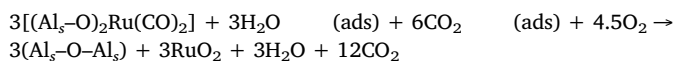


Fig. 1. PXRD patterns of (a) Ru(air), (b) Ru(H₂), and (c) Ru(N₂) samples with the reflections of Ru⁰ (PDF #06-0663), RuO₂ (PDF #43-1290), and γ -Al₂O₃ (PDF #10-0425) at the bottom.

with the minor reflections of γ -Al₂O₃ (PDF #10-0425). As revealed previously, the species [Ru(CO)₂X₂]_n is formed on Al₂O₃ surface by air oxidation at 20 °C or vacuum decomposition above 100 °C, where X represents an oxygen atom of the alumina lattice in this structure [27–41]. For the as-impregnated Ru₃(CO)₁₂/Al₂O₃ sample, IR bands were detected at 2073 and 2001 cm⁻¹ (Fig. S3), corresponding to Ru_B species among the reported Ru surface species. When the surface species (Al_s-O)₂Ru(CO)₂ is thermally decomposed in air, the reaction takes place as follows:



This reaction was confirmed by TGA result (Fig. S4) that the measured mass loss (13.0%) was very close to the theoretical mass loss (13.8%, calculated from the Ru loading and the mass loss of γ -Al₂O₃ at 800 °C) assumed to be valid.

Thermal decomposition in an air flow was investigated by TPD-MS experiment. Fig. 2a clearly shows CO₂ emission in the range 100–250 °C, which means that the prepared Ru(air) samples are free of Ru₃(CO)₁₂. This was in agreement with the FT-IR spectrum of Ru(air-400) sample exhibiting no IR bands of CO in the region 2200–1900 cm⁻¹ (Fig. S3). When the Hüttig and Tamman temperatures of RuO₂ (ca. 170 and 464 °C) are considered, larger RuO₂ particles would be formed by thermal decomposition in air at 400–700 °C. TPD-MS experiment also identified the release of H₂O (*m/z* = 18) in the range 100–250 °C by desorption of the adsorbed H₂O molecules.

Therefore, Ru(air) samples were reduced to Ru⁰ by H₂ at 250 °C for 3 h prior to the BPy hydrogenation reaction. Note that the reduction of RuO₂ is complete below 250 °C, confirmed by TPR experiments (Fig. S5). The reduced Ru(air) samples showed the BPy conversion of

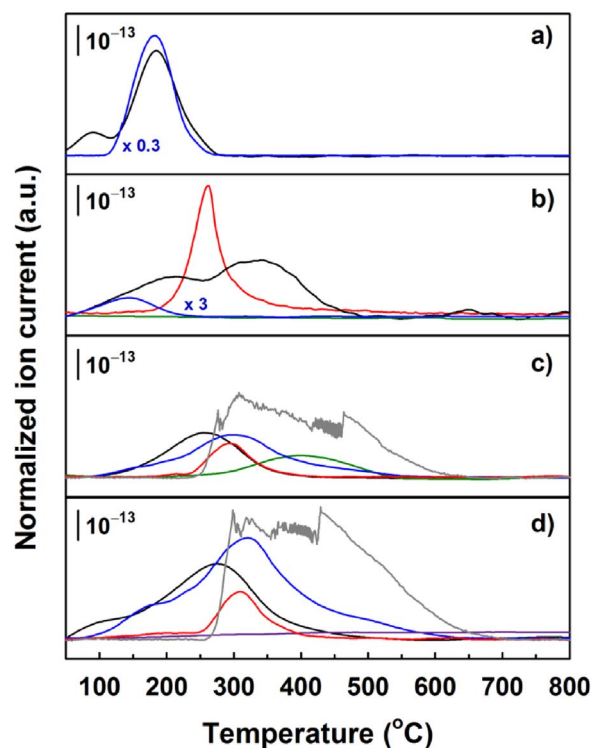


Fig. 2. Mass signals detected in the decomposition of the supported Ru precursor under (a) air, (b) H₂, (c) He, and (d) N₂, where the traces of *m/z* = 2, 18, 44, 16, 28, and 30 represent emission of H₂ (grey), H₂O (black), CO₂ (blue), CH₄ (red), CO (green), and NO/NO₂/N₂O (purple), respectively. (For interpretation of the references to colour in this figure legend, the reader is referred to the web version of this article.)

49–58% and the selectivity to CHPI of 63–74%, resulting in the H₂ storage efficiency of 40–50% (Table 1, entries 5–8). Their low activities are due to larger Ru⁰ particle sizes (i.e., lower Ru dispersions) found by CO chemisorption experiments. RuO₂ particles of large sizes were clearly observed in a high-magnification TEM image of Ru(air-500) (Fig. 3a).

In order to suppress the formation of large-sized RuO₂ particles, the supported Ru₃(CO)₁₂ was decomposed in air at 200 °C, yielding the Ru⁰ particle size of ca. 3.1 nm. However, the activity test showed the BPy conversion of 53.1%, CHPI selectivity of 75.9%, and H₂ storage efficiency of 46.6%, which is slightly lower than the activity of Ru(air-400). Since this is the unexpected result, Ru(air-200) was characterized by TPR-MS: a very huge TPR peak below 200 °C, similar to Ru(air-400), and additional hydrogen consumption around 350 °C (Fig. S6). In the accompanying mass traces of *m/z* = 15 for CH₄, the peak was detected around 350 °C. Since this was not detected for Ru(air-400), the result is explained by the fact that a little amount of carbonyl species still remains on the surface of Ru(air-200). Therefore, a low activation temperature under air favours the formation of smaller RuO₂ particles but leads to incomplete decomposition of carbonyl species.

3.2. Ru(H₂) samples prepared by thermal decomposition of the supported Ru₃(CO)₁₂ in H₂

For the samples subjected to H₂ activation at 400–700 °C, the typical reflections of γ -Al₂O₃ were only detected without Ru⁰-related reflections (PDF #06-0663) in the PXRD patterns (Fig. 1b). Thus, the as-prepared Ru(H₂) samples were tested in BPy hydrogenation without additional H₂ reduction. All Ru(H₂) samples exhibited the similar BPy conversion of ca. 89% and also the similar CHPI selectivity of 83 ± 1%, affording the enhanced H₂ storage efficiency of 82 ± 1% (Table 1, entries 9–12). Additionally, when Ru(H₂-500) was tested after reduction at 250 °C in the same manner as Ru(air) samples, the BPy

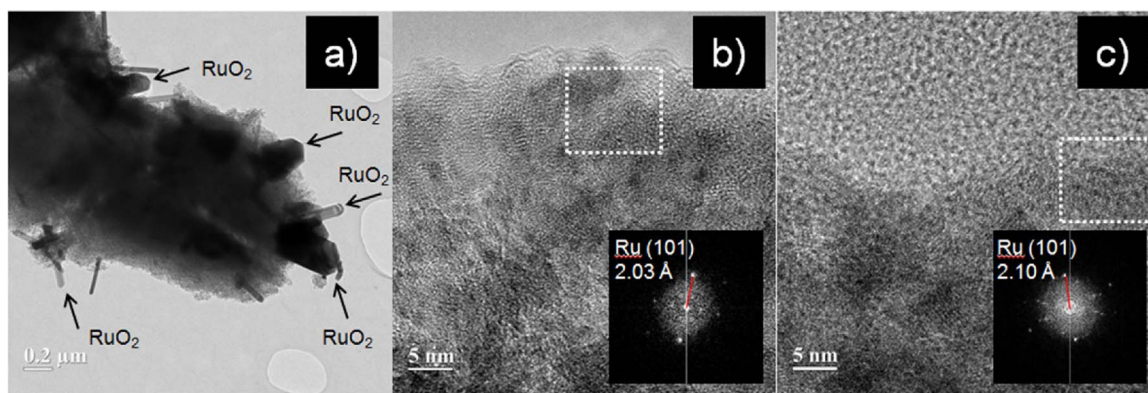
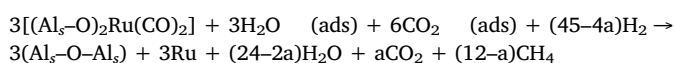


Fig. 3. High-resolution TEM images of the as-prepared samples; (a) Ru(air-500), (b) Ru(H₂-500), and (c) Ru(N₂-500).

hydrogenation activity was almost similar to that of the as-prepared Ru(H₂-500) (Table 1, entry 13). On the other hand, Ru(NO)(NO₃)₃ was used as Ru precursor and then Al₂O₃-supported Ru(NO)(NO₃)₃ was decomposed at 500 or 700 °C in H₂. The resulting samples exhibited a little lower performance (H₂ storage efficiency of ca. 69%) compared to the corresponding Ru₃(CO)₁₂-based ones (Table 1, entries 14 and 15). This is consistent to the previous results [24,25].

In thermal decomposition of the as-impregnated sample in a H₂ flow, the emission of CH₄ (*m/z* = 16) was observed in the range 200–400 °C (Fig. 2b). This is in agreement with no CO band in the region 2200–1900 cm⁻¹ for Ru(H₂-400) (Fig. S3). CH₄ is produced by direct methanation of carbon monoxide at discrete ruthenium sub-carbonyl sites. [29]. This explains no release of CO in TPD experiment. On the other hand, CO₂ emission was observed in the range 50–250 °C, which is related with the release of CO₂ adsorbed on the Ru-free part of Al₂O₃ surface. Also, H₂O was also emitted in the range 100–600 °C. H₂O emission at 100–250 °C is due to desorption of adsorbed H₂O molecules and the emission at 250–600 °C is possibly due to dehydroxylation of γ-Al₂O₃.

Based on the above results, it is presumed that the following reaction takes place in H₂:



For confirmation, separate TPR and TPO experiments were conducted for the as-prepared Ru(H₂) samples. The amount of H₂ consumed by TPR was calculated from the peak area in the range 50–150 °C (black curves in Fig. 4a). The low reduction degree of 14–25% for Ru(H₂) samples means the formation of Ru⁰ by decomposition of the supported Ru₃(CO)₁₂ in H₂. The weak H₂ reduction is explained by partial oxidation of Ru(H₂) samples by exposure to ambient air before use. This is confirmed by TPR experiments for the corresponding oxidized samples: a huge difference between black and red curves indicates the existence of Ru⁰ particles in Ru(H₂) samples (Fig. 4a). Additionally, the reduction degree decreases for both the as-prepared and oxidized samples as the activation temperature increases. This is due to strong interaction of unsaturated Ru⁰ atoms with the oxygen present in the alumina lattice [28]. TPO experiments for Ru(H₂-500) and Ru(H₂-700) also examined the formation of Ru⁰ particles by oxygen consumption from 250 to 550 °C (Fig. S7).

The sizes of supported Ru⁰ particles were calculated by CO chemisorption experiments for Ru(H₂) samples (Table 1). Ru⁰ particles of 1.5 ± 0.1 nm were found, which is associated with relatively high thermal stability of Ru⁰ (Hüttig temperature of 509 °C and Tamman temperature of 1031 °C). These much smaller Ru⁰ particles are responsible for the higher BPy hydrogenation activity compared to Ru(air) samples. Nanometer-sized Ru⁰ particles were confirmed in the TEM image of Ru(H₂-500) sample (Fig. 3b).

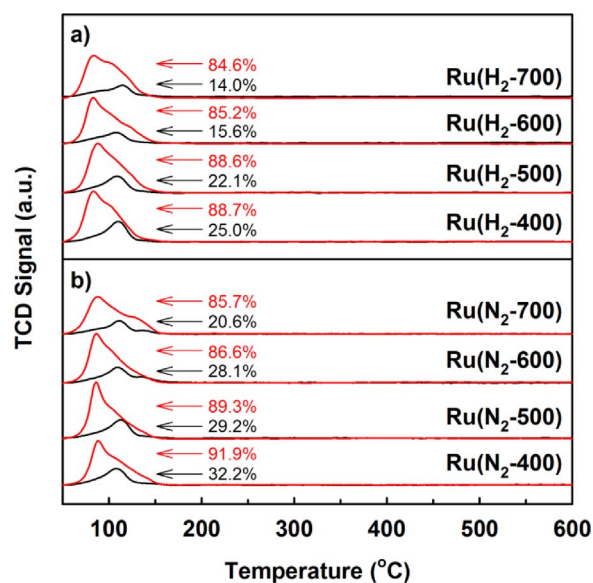


Fig. 4. Temperature-programmed reduction profiles of the as-prepared (a) Ru(H₂) and (b) Ru(N₂) samples (black curves), where TPR profiles of the samples oxidized in a 10% O₂/He flow at 400 °C for 1 h are added for comparison (red curves). The numerical values indicate the reduction degree of the samples. (For interpretation of the references to colour in this figure legend, the reader is referred to the web version of this article.)

3.3. Ru(N₂) samples prepared by thermal decomposition of the supported Ru₃(CO)₁₂ in N₂

PXRD patterns for the samples subjected to N₂ treatment at 400–700 °C are shown in Fig. 1c. In all patterns, Ru⁰-related reflections were not visible as for Ru(H₂) samples. However, very small reflections of RuO₂ (marked with red circles) were detected in the PXRD patterns of Ru(N₂-600) and Ru(N₂-700).

TPD-MS experiment was conducted in a He flow, where He instead of N₂ was used because CO has the same *m/z* of 28 as N₂. Along with the emission of H₂O and CO₂, CH₄ and CO emission were detected in the range 250–450 and 250–600 °C, respectively. The experiment in a N₂ flow also confirmed the CH₄ emission without any formation of NO, NO₂, and N₂O evidenced by the baseline mass trace of *m/z* = 30 (Fig. 2d). Basset et al. pointed out that the water on the hydrated η-Al₂O₃ support is the hydrogen source for CH₄ formation and it also takes parts in catalytic water gas shift reaction (CO + H₂O → CO₂ + H₂) explaining H₂ and CO₂ formation [27]. In terms of CH₄ formation, Bell et al. demonstrated that the reaction between the supported Ru₃(CO)₁₂ cluster and nucleophilic hydroxyl groups on the support surface occurs, resulting in the formation of ruthenium-hydride species that reacts with some fractions of CO in Ru surface species [28].

Although the exact chemical reaction could not be written due to complexity of the involved reactions, it is evident that highly dispersed Ru⁰ particles can be formed by thermal decomposition of the supported Ru₃(CO)₁₂ in N₂.

The observation of tiny amounts of RuO₂ in Ru(N₂-600) and Ru(N₂-700) by PXRD could be associated with strong interaction of coordinatively unsaturated Ru atoms with the oxygen present in the alumina lattice. This is supported by the fact that Ru–Ru bonds are broken and individual Ru atoms can be incorporated into the lattice to form surface RuAl₂O₄ [50] or RuAl alloys [51]. In order to search for another evidence for Ru incorporation, the supported Ru₃(CO)₁₂ was decomposed at 800 °C in N₂. As a result of activity test, the H₂ storage efficiency of Ru(N₂-800) was significantly dropped to 30.8% from 79.5% of Ru(N₂-500), where the nominal Ru loading was 5 wt.% (Fig. S8). This drop was also found for Ru(N₂-500) of 1 wt.% Ru nominal loading. The results are understood because larger Ru⁰ particles were produced at 800 °C. However, the PXRD pattern of Ru(N₂-800) reveals another clue for the activity decline: the reflections of γ-Al₂O₃ were significantly less intense and instead a very large hump was observed in the 2θ range 10–40°. The most related phase might be considered to be Ru₄Al₁₃ alloy (PDF #18-0056). This is believed to be a result of ruthenium incorporation into Al₂O₃, although further study is required for obtaining more direct evidences.

TPR and TPO experiments were also conducted for Ru(N₂) samples. The reduction degrees of the as-prepared Ru(N₂) samples were significantly different from those of the corresponding oxidized samples (Fig. 4b), as for Ru(H₂) samples. That is, Ru⁰ particles exist in the former Ru(N₂) samples. TPO experiments also showed the oxygen consumption from 250 to 550 °C (Fig. S7), elucidating the existence of Ru⁰ particles in Ru(N₂) samples.

In BPy hydrogenation the catalytic performance of Ru(N₂) samples was a little lower than or comparable to that of Ru(H₂) samples due to similar sizes of Ru⁰ particles (Table 1, entries 16–19). This indicates that for Ru(N₂) samples Ru⁰ nanoparticles would be dispersed well on the alumina support, which was confirmed in the TEM image of Ru(N₂-500) sample (Fig. 3c). It should be noted here that a very low amount of RuO₂ detected for Ru(N₂-600) and Ru(N₂-700) is reduced to Ru⁰ under the reaction condition. This was identified by the activity test over the reduced Ru(N₂-500) and Ru(N₂-700) samples showing only slightly lower H₂ storage efficiencies than the as-prepared ones (Table 1, entries 20 and 21).

3.4. Activity and stability comparison of Ru(air), Ru(H₂), and Ru(N₂) samples

Using the BPy conversions measured at the beginning of the hydrogenation reaction, the first-order rate constant (*k*) was estimated for Ru(H₂-500), Ru(N₂-500), and Ru(air-500) samples. Note that the first two samples were used as prepared whereas the last sample was reduced by H₂ at 250 °C for 3 h before use. Fig. 5 shows that Ru(H₂-500) and Ru(N₂-500) have very similar rate constants ($0.8 \pm 0.01 \text{ h}^{-1}$) which are 2.3-fold higher than 0.35 h^{-1} for Ru(air-500). These results are clearly explained with respect to the size of Ru⁰ particles: 13.4 nm for Ru(air-500) vs. 1.4 nm for Ru(H₂-500) and Ru(N₂-500). Additionally, we tried to compare the activities of Ru(H₂-500) and Ru(N₂-500) samples with different nominal Ru loadings of 1 and 3 wt.%. They were superior to the corresponding samples with 5 wt.% nominal loading, due to smaller Ru⁰ particle sizes (Table 1, entries 22–25). Also, there is very little difference between the activities of Ru(H₂-500) and Ru(N₂-500). In this regard H₂ or N₂ is recommended rather than air for thermal decomposition of the supported Ru₃(CO)₁₂.

Since catalyst stability is a very important issue in repeated hydrogen storage and release, the recycle runs were performed three times for Ru(H₂-500) and Ru(N₂-500) samples. Note that the recovered catalyst by filtration of the reaction mixture was used without any pre-treatment for the next run. The activity in the second run decreased by

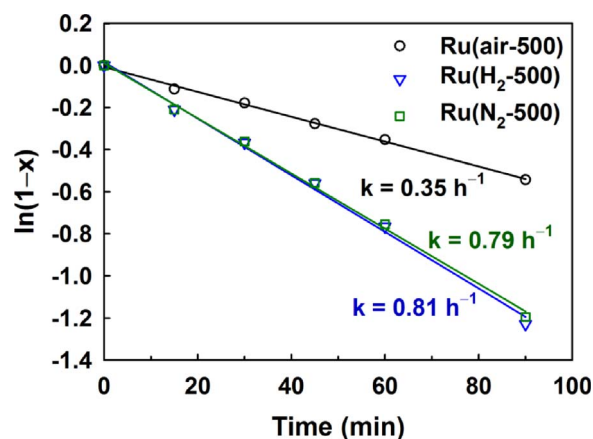


Fig. 5. Measurement for the rate constant in BPy hydrogenation over Ru(air-500), Ru(H₂-500), and Ru(N₂-500), where the rate dependence was assumed to be the first order in the substrate.

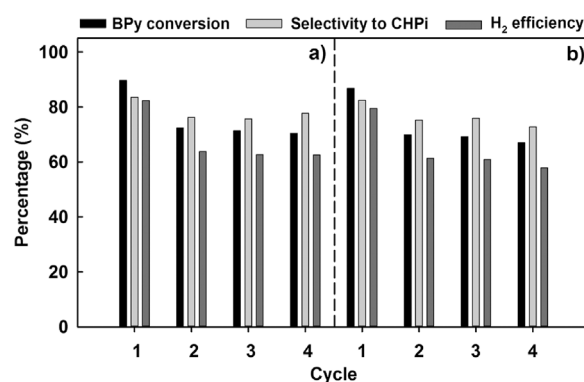


Fig. 6. BPy hydrogenation activities of (a) Ru(H₂-500) and (b) Ru(N₂-500) samples in the four repeated cycles.

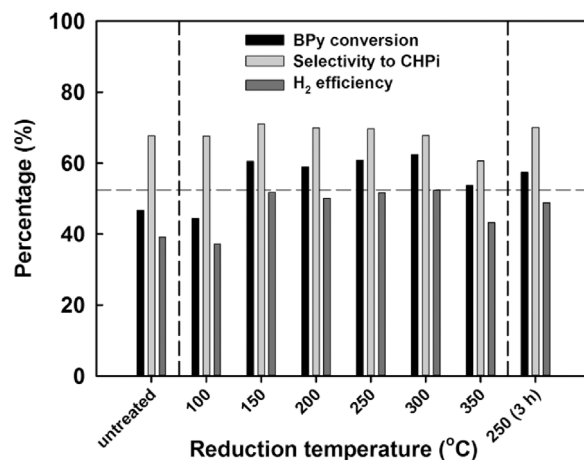


Fig. 7. BPy hydrogenation activities of Ru(air-500) samples subjected to different pre-treatments; the as-prepared sample (left section), the samples reduced at 100–350 °C for 30 min (middle section), and the sample reduced at 250 °C for 3 h (right section).

about 15% compared to the original activity, but the activity in further runs remained constant for both samples (Fig. 6). This indicates that Ru(H₂-500) and Ru(N₂-500) are relatively stable in the reaction although there is a little activity loss between the first and second runs. Therefore, the two samples are believed to be used repeatedly without pre-treatment for regeneration.

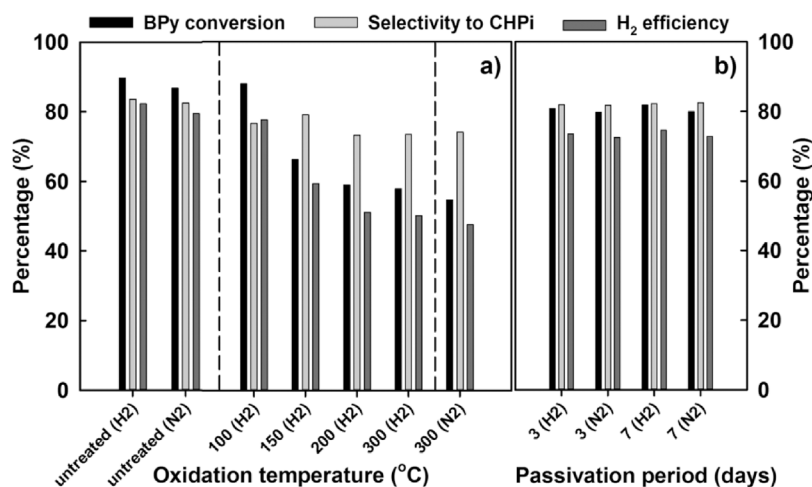


Fig. 8. BPy hydrogenation activities of Ru(H₂-500) and Ru(N₂-500) samples subjected to different pretreatments; (a) the as-prepared samples (left section), the Ru(H₂-500) samples oxidized at 100–300 °C for 30 min (middle section), and the Ru(N₂-500) sample oxidized at 300 °C for 30 min (right section), and (b) the Ru(H₂-500) and Ru(N₂-500) samples exposed under air at room temperature for 3 or 7 days.

3.5. Post-treatment of Ru(air), Ru(H₂), and Ru(N₂) samples

For Ru(air) samples, H₂ reduction should be conducted in order to transform RuO₂ into Ru⁰ active for the BPy hydrogenation. However, when the as-prepared Ru(air-500) sample was tested in BPy hydrogenation without pre-reduction, the H₂ storage efficiency was estimated to be 39.1%. Although the activity of the Ru(air-500) sample reduced at 250 °C for 3 h was higher than that of the as-prepared Ru(air-500), this means that some RuO₂ would be reduced to Ru⁰ under the hydrogenation reaction condition.

Thus, Ru(air-500) was reduced by pure H₂ for 30 min in the range 100–350 °C with the interval of 50 °C prior to the activity test (Fig. 7). Even though the 30-min reduction is assumed to be not enough for complete transformation of RuO₂ to Ru⁰, the samples obtained by reduction at 150–300 °C exhibited the comparable H₂ storage efficiencies (50.1–52.4%) to the Ru(air-500) sample reduced at 250 °C for 3 h. The lower hydrogenation activities of the reduced samples at 100 and 350 °C are a result of insufficient reduction of RuO₂ and sintering of Ru⁰ particles, respectively. Therefore, H₂ reduction would be conducted in the range 150–300 °C for at least 30 min prior to the hydrogenation activity test, when the supported Ru₃(CO)₁₂ is thermally decomposed in air.

On the other hand, Ru(H₂) and Ru(N₂) samples can be used as prepared, as confirmed in Table 1. However, if they are prepared ex-situ, the effect of oxidation condition needs to be investigated. When Ru(H₂-500) sample was oxidized in air at 100–300 °C for 30 min, the H₂ storage efficiency decreased from 82.3% for the as-prepared sample to 50.2% for the sample oxidized at 300 °C (Fig. 8a). This is absolutely due to the transformation of some Ru⁰ to RuO₂ by partial oxidation at high temperatures, which was similarly found for Ru(N₂-500) sample. Finally, Ru(H₂-500) and Ru(N₂-500) samples were exposed to ambient air for 3 or 7 days, and then tested in the BPy hydrogenation without additional H₂ reduction. This post-treatment is for addressing the stability of these samples. As shown in Fig. 8b, the H₂ storage efficiencies of the air-exposed samples were estimated to be 72.5–74.5%. The activity results were a little lower than those of the as-prepared samples but were significantly higher than those of Ru(H₂-500) samples pre-oxidized at 150–300 °C. This indicates that Ru(H₂-500) and Ru(N₂-500) samples are relatively stable under the ambient condition, although the prolonged exposure to air affects their hydrogenation activities in a little extent. This is also an evidence for strong interaction of Ru⁰ atoms with the oxygen in the alumina lattice.

4. Conclusions

From the superior catalytic performance and higher rate constant of Ru(H₂) and Ru(N₂) samples in BPy hydrogenation, it is believed that H₂

and N₂ are suitable atmospheres, compared to air, for thermal decomposition of Ru₃(CO)₁₂ supported on Al₂O₃. The activity enhancement is totally due to the formation of 1–2 nanometer-sized Ru⁰ particles in H₂ and N₂. This originates from direct hydrogenation of CO coordinated to the ruthenium surface complex in H₂ or selective methanation of the coordinated CO with ruthenium hydride species (formed by interaction between Ru–CO and nucleophilic hydroxyl groups on the support surface) in N₂. The so-obtained Ru⁰ particles in the as-prepared Ru(H₂) and Ru(N₂) samples are considered to be stable under ambient condition due to strong interaction between Ru⁰ atoms and the lattice oxygen in the alumina support. In contrast, RuO₂ is formed upon thermal decomposition of the supported Ru₃(CO)₁₂ in air. Due to high-temperature oxidation, RuO₂ particles become large and after H₂ reduction, Ru⁰ particles are larger than those in Ru(H₂) and Ru(N₂) samples. This explains lower activities of Ru(air) samples in BPy hydrogenation. Consequently, the results in this work will be utilized as useful recommendation towards preparing an active Ru catalyst by thermal decomposition of Ru₃(CO)₁₂ for the hydrogenation of N-containing compounds including BPy.

Acknowledgements

This research was financially supported by the Korea Institute of Energy Technology Evaluation and Planning under the Ministry of Trade, Industry & Energy, Republic of Korea (KETEP-2015-3030041160), as well as by the Basic Science Research Program through the National Research Foundation of Korea under the Ministry of Education, Republic of Korea (NRF-2016R1A6A1A03013422). The authors are grateful for partial support by the research fund of Hanyang University (HY-2011-00000000227).

Appendix A. Supplementary data

Supplementary data associated with this article can be found, in the online version, at <http://dx.doi.org/10.1016/j.apcata.2017.08.038>.

References

- [1] D. Teichmann, W. Arlt, P. Wasserscheid, R. Freymann, *Energy Environ. Sci.* 4 (2011) 2767–2773.
- [2] M. Markiewicz, Y.Q. Zhang, A. Bösmann, N. Brückner, J. Thöming, P. Wasserscheid, S. Stolte, *Energy Environ. Sci.* 8 (2015) 1035–1045.
- [3] K. Müller, J. Völkl, W. Arlt, *Energy Technol.* 1 (2013) 20–24.
- [4] T. He, Q. Pei, P. Chen, *J. Energy Chem.* 24 (2015) 587–594.
- [5] D. Geburtig, P. Preuster, A. Bösmann, K. Müller, P. Wasserscheid, *Int. J. Hydrogen Energy* 41 (2016) 1010–1017.
- [6] A. Moores, M. Poyatos, Y. Luo, R.H. Crabtree, *New J. Chem.* 30 (2006) 1675–1678.
- [7] N. Brückner, K. Obesser, A. Bösmann, D. Teichmann, W. Arlt, J. Dungs, P. Wasserscheid, *ChemSusChem* 7 (2014) 229–235.

- [8] F. Sotoodeh, B.J.M. Huber, K.J. Smith, *Appl. Catal., A: Gen.* 419–420 (2012) 67–72.
- [9] S. Lu, W.W. Loneragan, J.P. Bosco, S. Wang, Y. Zhu, Y. Xie, J.G. Chen, *J. Catal.* 259 (2008) 260–268.
- [10] R. Rahi, M. Fang, A. Ahmed, R.A. Sánchez-Delgado, *Dalton Trans.* 41 (2012) 14490–14497.
- [11] Y.P. Sun, H.Y. Fu, D.I. Zhang, R.X. Li, H. Chen, X.J. Li, *Catal. Commun.* 12 (2010) 188–192.
- [12] M. Tang, J. Deng, M. Li, X. Li, H. Li, Z. Chen, Y. Wang, *Green Chem.* 18 (2016) 6082–6090.
- [13] G.Y. Fan, J. Wu, *Catal. Commun.* 31 (2013) 81–85.
- [14] H. Greenfield, *Acad. Sci.* 214 (1973) 233–242.
- [15] L. Hegedüs, T. Máthe, A. Tungler, *Appl. Catal., A: Gen.* 147 (1996) 407–414.
- [16] K.M. Eblagon, D. Rentsch, O. Friedrichs, A. Remhof, A. Zuetzel, A.J. Ramirez-Cuesta, S.C. Tsang, *Int. J. Hydrogen Energy* 35 (2010) 11609–11621.
- [17] M. Freifelder, G.R. Stone, *J. Org. Chem.* 26 (1961) 3805–3808.
- [18] M. Freifelder, R.M. Robinson, G.R. Stone, *J. Org. Chem.* 27 (1962) 284–286.
- [19] J. Xu, X. Su, H. Duan, B. Hou, Q. Lin, X. Liu, X. Pan, G. Pei, H. Geng, Y. Huang, T. Zhang, *J. Catal.* 333 (2016) 227–237.
- [20] T.N. Phaahlamohlaka, D.O. Kumi, M.W. Dlamini, L.L. Jewell, N.J. Coville, *Catal. Today* 275 (2016) 76–83.
- [21] B. Lin, R. Wang, J. Lin, S. Du, X. Yu, K. Wei, *Catal. Commun.* 8 (2007) 1838–1842.
- [22] B. Lin, R. Wang, J. Lin, J. Ni, K. Wei, *Catal. Commun.* 12 (2011) 553–558.
- [23] D.A. Echeverri, J.M. Marín, G.M. Restrepo, L.A. Rios, *Appl. Catal., A: Gen.* 366 (2009) 342–347.
- [24] J. Álvarez-Rodríguez, A. Guerrero-Ruiz, I. Rodríguez-Ramos, A. Arcoya-Martín, *Catal. Today* 107–108 (2005) 302–309.
- [25] F. Lu, C. Yu, X. Meng, J. Zhang, G. Chen, P. Zhao, *RSC Adv.* 6 (2016) 73810–73816.
- [26] M. Shirai, Y. Murakami, N. Hiyoshi, N. Minura, A. Yamaguchi, O. Sato, *J. Mol. Catal. A: Chem.* 388–389 (2014) 148–153.
- [27] A.K. Smith, A. Theolier, J.M. Basset, R. Ugo, D. Commereuc, Y. Chauvin, *J. Am. Chem. Soc.* 100 (1978) 2590–2591.
- [28] V.L. Kuznetsov, A.T. Bell, Y.I. Yermakov, *J. Catal.* 65 (1980) 374–389.
- [29] D.A. Hucul, A. Brenner, *J. Am. Chem. Soc.* 103 (1981) 217–219.
- [30] A. Zecchina, E. Guglielminotti, A. Bossi, M. Camia, *J. Catal.* 74 (1982) 225–239.
- [31] E. Guglielminotti, A. Zecchina, A. Bossi, M. Camia, *J. Catal.* 74 (1982) 240–251.
- [32] E. Guglielminotti, A. Zecchina, A. Bossi, M. Camia, *J. Catal.* 74 (1982) 252–265.
- [33] J.G. Goodwin Jr., C. Naccache, *Appl. Catal.* 4 (1982) 145–152.
- [34] K. Asakura, M. Yamada, Y. Iwasawa, H. Kuroda, *Chem. Lett.* 14 (1985) 511–514.
- [35] Y. Iwasawa, *Adv. Catal.* 35 (1987) 187–264.
- [36] K. Asakura, Y. Iwasawa, M. Yamada, *J. Chem. Soc., Faraday Trans. 1: Phys. Chem. Condens. Phases* 84 (1988) 2457–2464.
- [37] K. Asakura, K.K. Bando, Y. Iwasawa, *J. Chem. Soc., Faraday Trans.* 86 (1990) 2645–2655.
- [38] K. Asakura, Y. Iwasawa, *J. Chem. Soc., Faraday Trans.* 86 (1990) 2657–2662.
- [39] S. Dobos, I. Böszörményi, V. Silberer, L. Guzzi, J. Mink, *Inorg. Chim. Acta* 96 (1985) L13–L15.
- [40] T. Mizushima, K. Tohji, Y. Udagawa, A. Ueno, *J. Am. Chem. Soc.* 112 (1990) 7887–7893.
- [41] E.E. Platero, F. Ruiz de Peralta, *Catal. Lett.* 48 (1997) 159–163.
- [42] X. Yang, W. Zhang, C. Xia, X. Xiong, X. Mu, B. Hu, *Catal. Commun.* 11 (2010) 867–870.
- [43] C. Yu, X. Meng, G. Chen, P. Zhao, *RSC Adv.* 6 (2016) 22633–22638.
- [44] J. Iwamoto, M. Itoh, Y. Kajita, M. Saito, K.I. Machida, *Catal. Commun.* 8 (2007) 941–944.
- [45] S. Muratsugu, S. Kityakarn, F. Wang, N. Ishiguro, T. Kamachi, K. Yoshizawa, O. Sekizawa, T. Uruga, M. Tada, *Phys. Chem. Chem. Phys.* 17 (2015) 24791–24802.
- [46] D. Szmigiel, W. Raróg-Pilecka, E. Miśkiewicz, M. Gliński, M. Kielak, Z. Kaszkur, Z. Kowalczyk, *Appl. Catal., A: Gen.* 273 (2004) 105–112.
- [47] K. Sato, K. Imamura, Y. Kawano, S.I. Miyahara, T. Yamamoto, S. Matsumura, K. Nagaoka, *Chem. Sci.* 8 (2017) 674–679.
- [48] J. Wang, H. Chen, Q. Li, *React. Kinet. Catal. Lett.* 69 (2000) 277–284.
- [49] M. Trueba, S.P. Trasatti, *Eur. J. Inorg. Chem.* 17 (2005) 3393–3403.
- [50] L. Yongxue, W. Shuguang, Y. Pinliang, X. Qin, *React. Kinet. Catal. Lett.* 40 (1989) 53–58.
- [51] O. Okada, M. Ipponmatsu, M. Kawai, K. Aika, T. Onishi, *Chem. Lett.* 13 (1984) 1041–1044.